GRAFTING CHITOSAN WITH MALEIC ANHYDRIDE AND VINYL BENZYL CHLORIDE: A ROUTE TO ENHANCED FUNCTIONAL POLYMERS

Oana-Maria MEMECICĂ[1], Ileana RĂU[1], Gabriela PERCA[2], Cristi Andi NICOLAE[3]

The graft copolymerisation of chitosan with 4-vinyl benzyl chloride (VBC) and maleic anhydride (MA) was performed using cerium (IV) sulfate (Ce (SO4)2) as an initiator to enhance the physicochemical properties of the biopolymer. The efficiency of the grafting process was analysed through Fourier-transform infrared spectroscopy (FTIR), Raman spectroscopy, and thermogravimetric analysis (TGA). The Raman spectra revealed significant structural changes, particularly in the vibrational modes associated with amine, carbonyl, and aromatic functionalities, confirming the successful grafting of both VBC and MA onto chitosan. FTIR analysis supported these findings by identifying the characteristic peaks. TGA provided further evidence of polymer modification through the changes in the thermal degradation behaviour of grafted chitosan, with an improved thermal stability in the presence of VBC. The study confirms that the grafting efficiency is primarily influenced by the monomer ratios and the reactivity of VBC, which exhibited a higher polymerisation yield compared to MA. These results contribute to advancing functionalised chitosan materials with potential applications in biomedicine, drug delivery, and environmental remediation.

Keywords: Chitosan, graft copolymerisation, 4-vinyl benzyl chloride, maleic anhydride, $Ce(SO_4)_2$, FTIR, Raman spectroscopy, TGA, polymer modification, thermal stability

1. Introduction

Chitosan, a natural polysaccharide derived from chitin, has garnered significant attention due to its biocompatibility, biodegradability, and functional versatility, making it a valuable candidate for biomedical, pharmaceutical, and environmental applications [1]. However, its inherent solubility liimpliesions and

[1] Department of General Chemistry, Faculty of Chemical Engineering and Biotechnology, National University of Science and Technology POLITEHNICA Bucharest, Romania, e-mails: maria.memecica@yahoo.com (corresponding author), ileana.rau@upb.ro

[2] Department of Bioresources and Polymer Science, Faculty of Chemical Engineering and Biotechnology, National University of Science and Technology POLITEHNICA Bucharest, Romania, e-mail: gabriela.perca@yahoo.com

[3] Department of Polymers, National Institute of Research and Development in Chemistry and Petrochemistry, Bucharest, Romania, e-mail: cristian.nicolae@icechim-pd.ro

relatively low chemical reactivity imply structural modifications to enhance its functional potential [2]. One of the most effective approaches to achieving this goal is graft copolymerization, which introduces functional monomers onto the chitosan backbone to tailor its physicochemical properties for targeted applications [3].

Among the monomers explored for chitosan modification, maleic anhydride (MA) and 4-vinyl benzyl chloride (VBC) exhibit complementary reactivity and potential to form charge-transfer complexes [4]. MA, a well-known electron acceptor, is frequently used in polymer modifications but tends to form oligomers due to its limited polymerization reactivity [5]. In contrast, VBC, a potent electron donor, has high polymerization efficiency and enhances the grafting process when combined with MA [6]. This study aims to investigate the graft copolymerization of MA and VBC onto chitosan using $Ce(SO4)2$ as a redox initiator, by evaluating the effects of monomer ratios, reaction conditions, and by solvent media on the efficiency and characterizing the modified polymer [7].

A combination of FTIR, Raman spectroscopy and TGA analyses was conducted to evaluate the structural and thermal properties of the grafted chitosan comprehensively. The study examines how variations in monomer ratios and reaction conditions influence the grafting yield, providing insight into the optimal conditions for maximizing polymer modification [8]. The findings of this study contribute to the broader understanding of chitosan modification strategies and their implications in the development of advanced biomaterials and functional polymers.

2. Materials and methods

Medium molecular weight chitosan with a degree of deacetylation of 75-85% and a molecular weight between 190 – 310 kDa was purchased from Sigma-Aldrich and used as supplied as a substrate for graft polymerisation. $Ce(SO4)2$ anhydrous was purchased from Sigma-Aldrich and used as an initiator for the grafting polymerisation without further purification. 4-vinyl benzyl chloride (VBC) (mixture of 3 and 4- 4-isomers, 97% purity) monomers was purchased from Sigma-Aldrich and used without further purification. Maleic anhydride (MA) monomer was procured in the form of briquettes from Sigma-Aldrich and used after cleansing by recrystallization from $CHCl3$. 1,4-Dioxane anhydrous of 99.8% purity (Sigma-Aldrich), toluene of 99% purity (Chimopar S.A.), sulfuric acid in 98%w/w (Sigma-Aldrich), and acetone of 99.92% (Chimreactiv SRL) were used as supplied. Whatman® cellulose thimbles (10 mm × 50 mm) were obtained from Sigma Aldrich and utilised in the purification of the products by Soxhlet extraction after drying to constant mass.

2.1. FTIR Analysis

The infrared analysis was performed using a spectrometer from Interspectrum (Interspec 200-X FTIR Spectrometer) over the frequency range of 4000 ÷ 500 cm^{-1}. Each sample of chitosan was dried before mixing it with previously dried KBr, then pressed to obtain a KBr based disc.

2.2. Thermogravimetric analysis (TGA)

TGA was performed using Thermogravimetric Analyzer TGA Q5000IR to evaluate the thermal stability of the grafted chitosan samples. The samples were heated from room temperature to 1000°C under a synthetic air atmosphere at a heating rate of 10°C/min. The thermal degradation parameters were determined, including the onset temperature, weight loss percentage, and residue at high temperatures. The data obtained provided insights into the impact of graft copolymerisation on chitosan's thermal behaviour

2.3. Raman spectroscopy

Raman spectra were recorded using a Renishaw inVia Raman Spectrometer with a 532 nm laser and a 50× objective lens. The spectral range was 1800-100 cm^{-1}, with an integration time of 10 s per scan and 10 accumulations per sample. The laser power was set to 10 mW to prevent thermal degradation. Calibration at 520 cm^{-1} was performed using a silicon reference.

Key spectral features analyzed included NH_2 bending, C=O stretching, and aromatic ring vibrations to confirm successful grafting. The spectral shifts and intensity variations validated the chemical interactions between chitosan and the grafted monomers.

2.4. Experimental procedure

Table 1

Molar composition of the synthetised compounds

Compound	Mp(°C)	Formula	N(%)	
			Calc.	Found
3A	178	$C_{29}H_{34}N_2O$	6.57	6.70
3B	264	$C_{29}H_{33}N_3O_3$	8.92	8.85
3C	232	$C_{29}H_{32}N_4O_5$	10.85	10.78
5A	185	$C_{29}H_{34}N_2O$	6.56	6.41
5B	242	$C_{29}H_{33}N_3O_3$	8.92	8.87
5C	245	$C_{29}H_{32}N_4O_5$	10.85	10.63

Due to its high efficiency, the grafting polymerisation of MA, grafting homopolymerisation of VBC and grafting copolymerisation of MA and VBC were performed on chitosan pre-treated with Ce(SO4)2 for 20 minutes.

A known mass of chitosan pre-treated with Ce(SO4)2 was dispersed in 10 mL of dioxane. Subsequently, MA (for MA homopolymerisation), VBC (for VBC

homopolymerisation) or a mixture 1:1 of MA and VBC (for the copolymerisation of MA and VBC) were introduced in the reaction vessel at concentration of 0.5 mole/L and molar ratios as shown in **Table 1**. The grafting copolymerisation of MA and VBC was performed under a nitrogen atmosphere using toluene as dispersion medium, a temperature of 35°C and continuous moderate stirring for few hours. The initial time of the reaction was considered the moment at which the monomer/all monomers were added to the reaction tube. After polymerisation, the chitosan substrate was washed with acetone, dried at low pressure for 24 h, and then purified using acetone in a Soxhlet apparatus. Further, the product was dried under vacuum to a constant weight.

3. Results

3.1. Grafting efficiency

The grafting was firstly studied in the case of MA or VBC alone. The grafting process was studied using different molar ratios (Table 1). From **Fig. 1**, one can see the influence of the monomer, VBC leading to higher rates as compared to MA monomer. This finding is not surprising given the nature and the behaviour of the two monomers in polymerisation. While MA is an acceptor with reactivity limited to the formation of oligomers with 2-5 monomer units, VBC is a donor-type monomer with high polymerisation reactivity. It should be noted that the molar ratio between the monomer and the aminoglycoside units in chitosan determines the grafting yield.

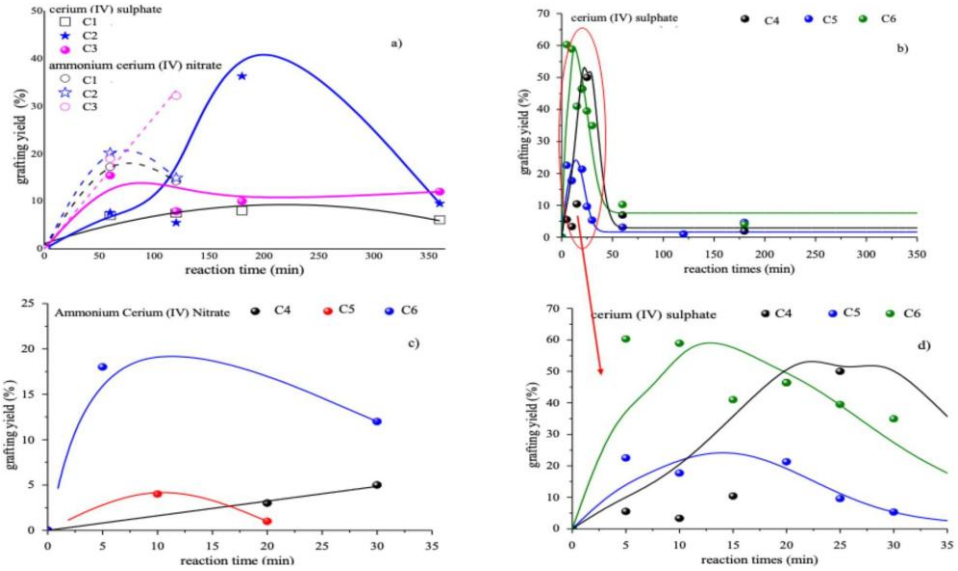

Fig. 1. Evolution of the overall grafting yield of chitosan with MA (a); VBC using $Ce(SO_4)_2$ as initiator (b); VBC using cerium (IV) nitrate as initiator (c) and details for grafting yield of chitosan with VBC using $Ce(SO_4)_2$ as initiators (d)

In the case of maleic anhydride (MA) (Fig. 1a), the highest grafting yield (~41%) is obtained at an equimolar monomer-to-glycosidic unit ratio (C2). Both sub-stoichiometric (C1) and supra-stoichiometric (C3) ratios result in significantly reduced yields, with values of approximately 10% and 14%, respectively. These results suggest that optimal grafting efficiency for MA occurs at a specific concentration threshold, likely due to the formation of a transient energetic complexes between MA and the reactive sites from chitosan. This intermediate state appears to be concentration-dependent and enables efficient propagation of grafted chains under equimolar conditions.

Vinylbenzyl chloride (VBC) (Fig. 1b) exhibits distinct behavior, achieving its highest grafting efficiency (~60%) within the first 15 minutes at a 2:1 monomer-to-chitosan molar ratio (C6). This reflects VBC's high reactivity and donor character during radical propagation. At equimolar (C5) and sub-stoichiometric (C4) monomer-to-chitosan ratios, grafting efficiencies are lower—around 50% and 24%, respectively—and the reaction proceeds more slowly, although moderate grafting still occurs.

Despite these differences in grafting yield, the overall monomer conversion remains high for both monomers, particularly MA. This further supports the existence of parallel reactions, especially homopolymerization in the aqueous phase, which reduces the effective grafting efficiency by consuming the monomer outside the chitosan matrix.

Taken together, these findings highlight that grafting performance is determined not only by monomer reactivity but also by the stoichiometric balance between monomer and polysaccharide substrate. For highly reactive monomers such as VBC, a molar excess accelerates the reaction and maximizes the grafting yield over short durations. For less reactive monomers such as MA, efficient grafting is best achieved at equimolar conditions where molecular interactions are optimized. Therefore, selecting an appropriate monomer-to-glycosidic unit ratio—preferably in favor of the monomer—enables both higher grafting efficiencies and reduced reaction times, which are advantageous for potential scale-up and application in functional biomaterials.

Fig. 1a reveals the evolution of MA effiiency grafting in time highlighting the strong influence of initiators. Thus the grafting experiments also differentiated the initiation efficacy of $Ce(SO_4)_2$ compared to the classic cerium ammonium nitrate. As it can been seen from the comparative evolution of grafting yields when using the two types of cerium initiators, a higher efficiency was obtained when $Ce(SO_4)_2$ was used.

In the case of the grafting chitosan with MA-VBC copolymer (Fig. 2), it is observed a similar evolution with the VBC's grafting in all cases. In addition, in all three compositional cases for VBC's grafting, the yield increases by 18-22% (78%

for compound C6 at 15 minutes of reaction, 46% for compound C5 at 8 minutes, and 27% for compound C4 at 30 minutes). This behaviour shows the formation by grafting of a complex with increased reactivity. Considering the nature of the two monomers, the idea of forming a charge transfer complex specific to donor-acceptor monomer pairs emerges.

Figs. 2 and 3 show the grafting yield evolution in time and the monomers/copolymer conversion in the chitosan grafting process for different molar ratios monomer/copolymer: glycosidic units.

As expected, increasing the molar ratio, the grafting yield is increasing while the reaction time is decreasing. The highest grafting yield was obtained for compound C9. Another important observation is represented by the fact that the value of the grafting yield is given by the presence of VBC monomer.

If the evolution of the overall monomer conversion is compared to that of the grafting yield, one can see that there are similar behaviours except the cases in wich MA was used as monomer or in mixture with VBC. In this last case, the evolution of overall monomer conversion during the grafting reactions reveals a trend opposite to that of grafting yield. This observation can be attributed to the limited accessibility of the monomer to the reactive sites along the chitosan backbone. Such steric and diffusional constraints tend to favor alternative reaction pathways, notably the solubilisation of short chitosan sequences and the homopolymerization of the monomer within the dispersion medium. As a consequence, an important fraction of the monomer is consumed without contributing to grafting process.

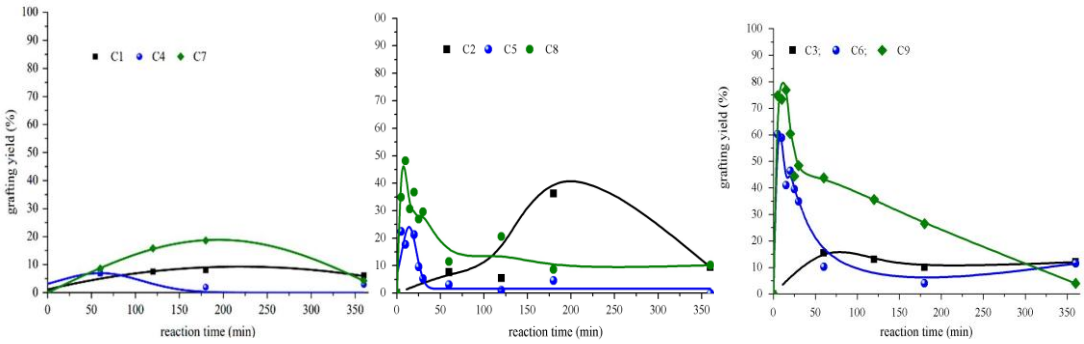

Fig. 2. Evolution of the overall grafting yield of chitosan with AM, VBC, AM:VBC

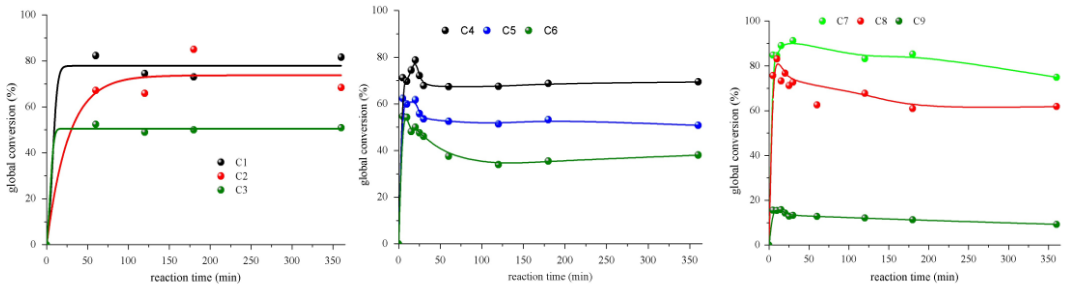

Fig. 3. Evolution of the overall conversion in the grafting of chitosan with MA, VBC, and MA-VBC

3.1. FTIR Analysis

To confirm the grafting on chitosan with MA, VBC homopolymer and their copolymer, FTIR Spectroscopy was used. FTIR spectroscopy may indicate possible structural changes in the substrate after the grafting polymerisation.
The FTIR spectra of pure chitosan (CS) and Ce(SO4)2-treated chitosan (CE) are shown in Fig. 4.

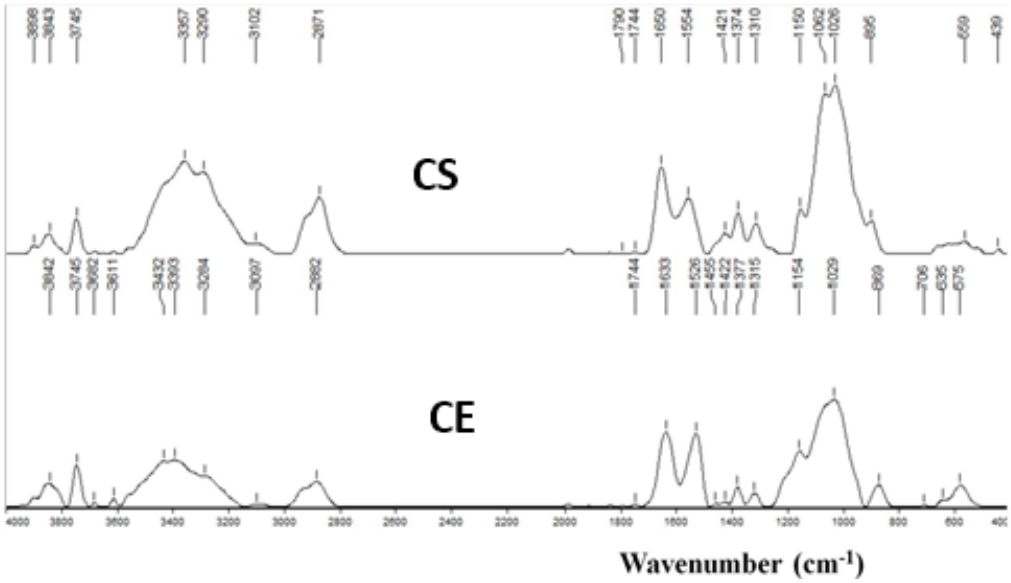

Fig. 4. FTIR spectra for pure chitosan (CS) and $Ce(SO_4)_2$-treated chitosan (CS-CE)

From the FTIR spectra of pure chitosan and $Ce(SO_4)_2$ -treated chitosan, it can be noticed that the treatment of chitosan with $Ce(SO_4)_2$ leads to a decrease in the intensity of the peak at 3357 cm^{-1} corresponding to the stretching vibrations of the N-

H bonds from the primary amine groups of chitosan and its shift towards 3393 cm^{-1}. At the same time a decrease in the intensity of the peak at 3290 cm^{-1} assigned to the stretching vibrations of the O-H bonds from the hydroxyl (OH) groups of chitosan together with its shift to 3284 cm^{-1} can be observed. Similarly a reduction in the intensity of the band observed at 2871 cm^{-1} which corresponds to the C–H stretching vibrations from the methyl ($-CH_3$) groups from chitosan together with its shift to 2882 cm^{-1} can be seen. These changes suggest that after the treatment of chitosan with $Ce(SO_4)_2$, the disappearance of some of the $-NH_2$ and OH groups involved in establishing hydrogen bonding interactions in chitosan may occur, and by consequence a redistribution of the hydrogen bonds inside the material could take place. In other words it can be affirmed that some -NH2 and -OH groups from chitosan will no longer be involved in establishing hydrogen bonding interactions as they are bind the Ce^{4+} ions through coordinative bonds. Other changes in the IR spectrum of CE which confirm the interaction between chitosan and Ce(SO4)2 are represented by the intensity equalization of the peaks at 1650 cm^{-1} and 1554 cm^{-1} corresponding to the C=O stretching vibration from amide I and N-H stretching vibration from amide II and their shift to lower wavenumber of 1633 cm^{-1} and 1554 cm^{-1}. Moreover the presence of the band at 635 cm^{-1} which can be attributed to the S=O or S–O stretching vibrations from the sulphate ($SO4^{2-}$), confirms also the binding of $Ce(SO_4)_2$ to chitosan [8]. The peak at around 575 cm^{-1} from the $Ce(SO_4)_2$ -treated chitosan may be associated with the Ce–N vibrations arising from the coordination bond between cerium and the nitrogen atoms. All this spectroscopic evidence strongly indicates the formation of a complex compound between chitosan and the Ce^{4+} cations. The FTIR analysis was also performed on chitosan after the grafting, as shown in Fig. 5.

The most important structural changes can be seen in the spectrum of CE modified by the grafting polymerisation of MA (CE-MA). The band at 1711 $cm^{-1,}$ which is characteristic for the symmetric C=O stretching vibration from anhydride, represent a proof of the grafting of MA on chitosan chains. In addition, the widening of the peak at 1027 cm^{-1} which can be assigned to the inclusion of the stretching vibrations of the C-O-C bonds from MA in the band characteristic to the stretching vibrations C-O-C of chitosan may indicate that MA attachment to the chitosan chains took place.

The spectra corresponding to chitosan grafted with poly(VBC) and poly(MA-co-VBC), respectively, are very similar to those of chitosan treated with $Ce(SO_4)_2$. Therefore no structural-compositional changes that occur in the substrate after grafting polymerisation can be identified. The peaks that could indicate the structural modifications occurring after grafting overlap with the peaks characteristic of chitosan treated with $Ce(SO_4)_2$. substracted from the chitosan spectrum grafted with poly(VBC).

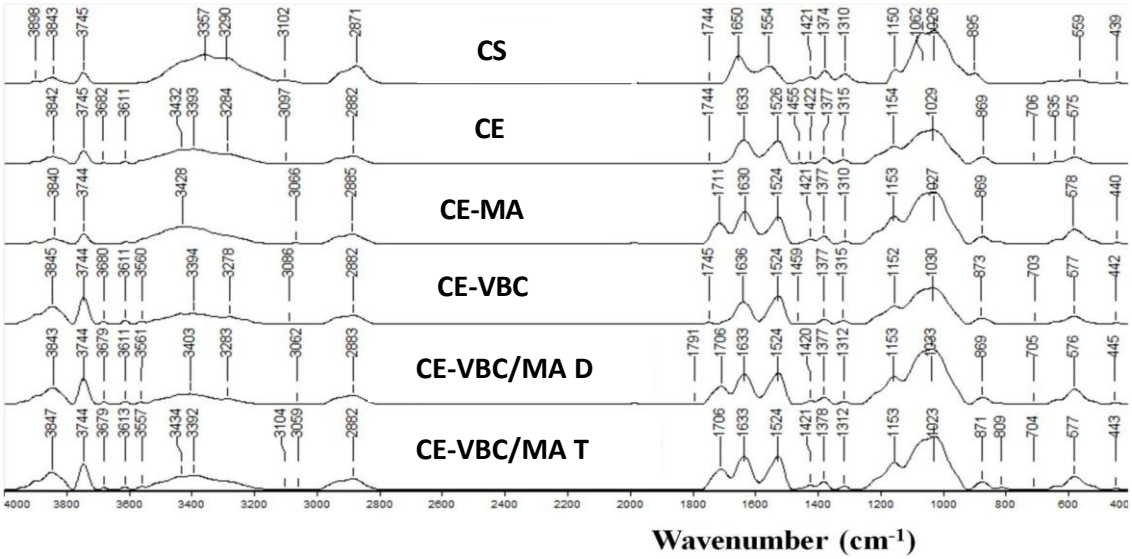

Fig. 5. Comparative FTIR spectra for pure chitosan (CS), cerium chitosan treated (CE) and obtained materials by grafting (co) polymerization, (CE-MA, CE-VBC), co-polymerization of cerium treated chitosan with VBC and MA in dioxan as a solvent(CE-VBC/MA D), co-polymerization of cerium treated chitosan with VBC and MA in toluene as a solvent (CE-VBC/MA T)

Therefore to identify these structural changes the $Ce(SO_4)_2$ treated chitosan interfering spectrum was substracted from the chitosan spectrum grafted with poly(VBC).

The weak peak at 3136 cm^{-1} can be attributed to the C–H stretching from the aromatic rings of the grafted poly(VBC). The peaks at 2918 cm^{-1} and 2853 cm^{-1} are assigned to the asymmetric and symmetric C-H stretching vibration of the aliphatic $-CH_2-$ groups and can be attributed to the multitude of $-CH_2-$ groups formed following the VBC homopolymerisation. The peaks at 1918 cm^{-1} and 1837 cm^{-1} are characteristic to the 1,4-disubstituted aromatic ring vibrations. The absorption band at 1511 cm^{-1} belongs to stretching vibrations of C=C bonds from the aromatic ring present in poly(VBC). The peak at 1024 cm^{-1} corresponds to the stretching vibration of C-H from the aromatic ring [9] while the band at 979 cm^{-1} can be assigned to the stretching vibration of the methylene chloride group (CH_2-Cl) from poly(VBC). The bands at 1282 cm^{-1} and 911 cm^{-1} are specific to the S-O bond vibrations, and suggests an interaction of the $Ce(SO_4)_2$ with the biopolymer through a bidentate complex (in which two atoms from the structure of chitosan are involved: O from the OH group from the C-3 carbon and -N from $-NH_2$ group from position C-2).

To be able to elucidate the structural changes that occur in the $Ce(SO_4)_2$-treated chitosan after the grafting copolymerisation of MA and VBC, the interfering spectrum of $Ce(SO_4)_2$-chitosan was subtracted from the chitosan grafted with poly(MA-co-VBC) in 1,4-dioxane and toluene spectra.

In the FTIR spectra of chitosan after the grafting copolymerisation of MA and VBC, a band can be observed at 1700/1709 cm^{-1}, which may be assigned to the symmetric stretching vibrations of the C=O bond from the anhydride group. The peak at 1408/1410 cm^{-1} can be assigned to the stretching vibrations of the C=C bonds from the aromatic ring of VBC. The peak at 1149 cm^{-1} may be attributed to the C-H wagging vibrations from the -CH_2Cl group of VBC while the 928/935 cm^{-1} bands can be assigned to the methylene chloride bond stretching vibration (CH_2-Cl) from poly(VBC). Interestingly, the use of dispersion enviroment with different polarity, i.e., 1,4-dioxane and toluene, determined some peculiarities of structure in the grafted copolymer, which are visible in the FTIR spectra. Thus, when 1,4-dioxane is used as a dispersion enviroment, a wide band at 1056 cm^{-1} which may be assigned to the C-O-C stretching vibrations from MA and C-O-C stretching vibrations from the glycosidic ring is observed. When toluene is used as a solvent, the band corresponding to these bonds splits into a peak at 1016 cm^{-1} and a shoulder at 1063 cm^{-1}, which practically sets a delimitation between the bands corresponding to the C-O-C stretching vibrations from MA and C-O-C stretching vibrations from the glycosidic ring of chitosan. There is also a change in the ratio between the intensity of the absorption peak characteristic to MA (the peak from 1700/1709 cm^{-1} attributed to the C=O bond in the maleic anhydride cycle) and the absorption peak characteristic to VBC (the peak from 928/935 cm^{-1} for the CH_2-Cl group in VBC) from 23 in 1,4-dioxane to 22 in toluene.

The grafting of maleic anhydride (MA) and vinylbenzyl chloride (VBC) onto chitosan is proposed to occur via a free radical mechanism initiated by $Ce(SO_4)_2$, as illustrated in Scheme 1. In this pathway, Ce(IV) selectively abstracts hydrogen atoms from the amino ($–NH_2$) and hydroxyl (–OH) groups of chitosan, primarily at the C2 and C3 positions of the glucosamine unit, leading to the formation of macroradicals. These radical centers serve as active sites for the propagation of MA and VBC chains, resulting in grafted copolymers covalently attached to the chitosan backbone.

Interestingly, no bands associated with newly formed aldehyde (CH=O) or imine (C=NH) groups were detected in the spectra, suggesting that the grafting does not proceed through oxidation or condensation pathways. Instead, the radical mechanism described in Scheme 1 is more likely, involving direct monomer addition at the active sites generated by Ce(IV) on the chitosan chain.

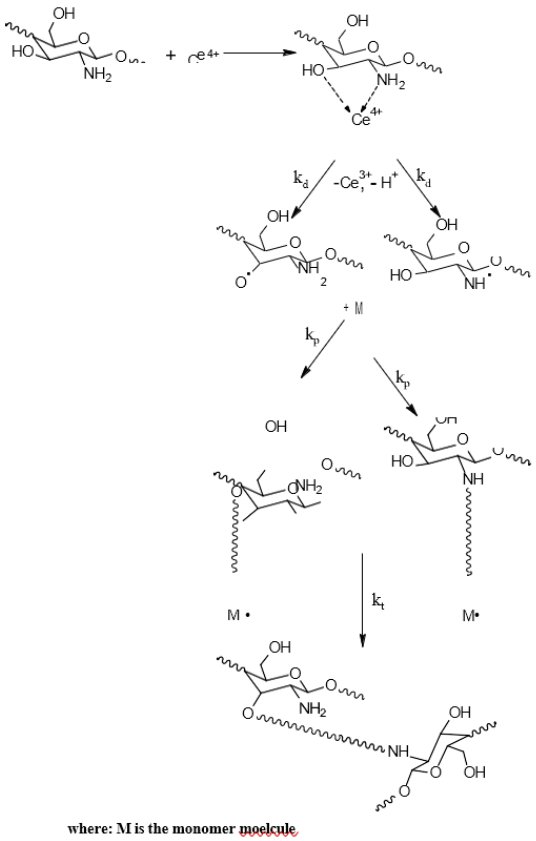

Scheme 1. Possible mechanism of homopolymerisation/copolymerisation of MA and VBC on chitosan

3.2 Thermogravimetric analysis (TGA)

The thermal stability of chitosan after its chemical modification by the grafting homopolymerisation/copolymerisation on its chains of MA and VBC was characterised by thermogravimetric analysis (TGA). Thermal parameters such as the temperature corresponding to the maximum degradation rate of each thermal degradation step (T_{max}), the initial temperature (T_0) at which each thermal degradation step begins, the weight loss (Δm) and the residue at 1000°C for pure chitosan, Ce(SO4)2-treated chitosan and chitosan modified by grafting homopolymerisation/copolymerisation with MA and VBC are given in Table 2.

The TGA curves were recorded for chitosan modified by grafting homopolymerisation of MA, grafting homopolymerisation of VBC, grafting copolymerisation of MA and VBC in 1,4-dioxane and grafting copolymerisation of MA and VBC in toluene.

Table 2

Thermal parameters chitosan modified by the copolymerisation of MA - VBC obtained from the thermogravimetric analysis performed in air atmosphere

SAMPLE	STEP 1			STEP 2			STEP 3			STEP 4			STEP 5		
CE-MA	T_0 (°C)	T_{max} (°C)	Δm (%)	T_0 (°C)	T_{max} (°C)	Δm (%)	T_0 (°C)	T_{max} (°C)	Δm (%)	T_0 (°C)	T_{max} (°C)	Δm (%)	T_0 (°C)	T_{max} (°C)	Δm (%)
	-	57.34	11.49	149.09	248.28	46.7	366.85	436.25	13.29	456.09	518.75	23.59	637.96	721.56	1.78
	Residue at 1000°C (%): 3.15														
CE-VBC	STEP 1			STEP 2			STEP 3			STEP 4			STEP 5		
	T_0 (°C)	T_{max} (°C)	Δm (%)	T_0 (°C)	T_{max} (°C)	Δm (%)	T_0 (°C)	T_{max} (°C)	Δm (%)	T_0 (°C)	T_{max} (°C)	Δm (%)	T_0 (°C)	T_{max} (°C)	Δm (%)
	-	54.25	12.51	153.76	253.12	43.35	352.16	435.74	16.36	460.5	524.57	23.05	640.02	679.48	1.24
	Residue at 1000°C (%): 4.49														

CE-MA: chitosan modified by graft polymerisation of MA; CE-VBC: chitosan modified by graft polymerisation of VBC

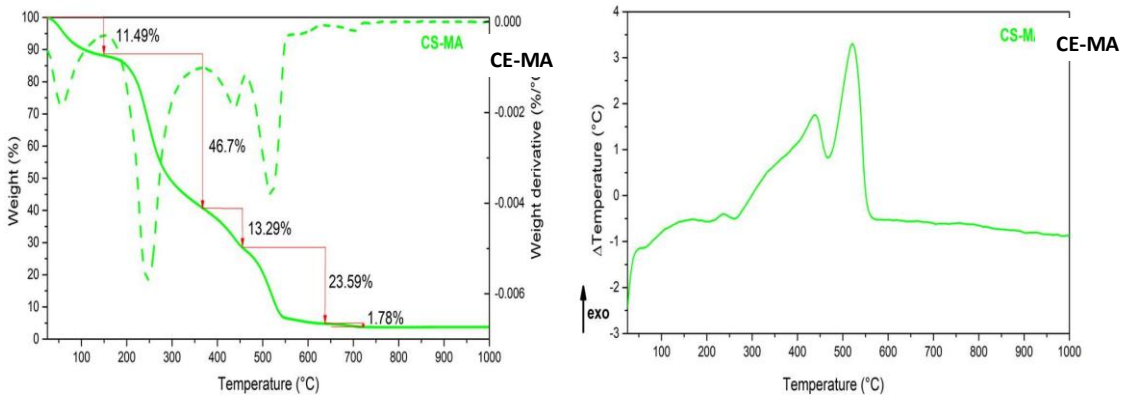

Fig. 6. The thermogravimetric (TG), derivative thermogravimetric (DTG) and differential thermal analysis (DTA) curves of chitosan modified by grafting homopolymerisation of MA (CE-MA)

As it can be observed from Figs. 6-12 and table 2, the thermal degradation of chitosan modified by the grafting homopolymerisation of MA, grafting homopolymerisation of VBC and grafting copolymerisation of MA and VBC in both 1,4-dioxane and toluene is very similar to that of Ce(SO4)2-treated chitosan, suggesting that the chemical modification of chitosan with the polymers/copolymers of MA and VBC does not significantly modify the chitosan thermal stability, maybe due to the small amount of polymer/copolymer grafted on chitosan. Thus, the main reason for the decrease in the thermal stability remains the pre-treatment with Ce(SO4)2.

As it can be seen from table 2, up to 153.76°C, chitosan grafted with the homopolymers/copolymer of MA and VBC suffers a first thermal degradation step which can be assigned to the removal of chemically and physically bound water as well of the potential residual solvents from materials. As compared to pure chitosan, all chitosan samples modified by grafting polymerisation show a more significant weight loss in this first step of thermal degradation as compared to pure chitosan (7.74% for pure chitosan *vs.* 11.49%, 12.51%, 10.62% and 10.06% for chitosan modified by the grafting homopolymerisation of MA, grafting homopolymerisation of VBC, and grafting copolymerisation of MA and VBC in 1,4-dioxane and grafting copolymerisation of MA and VBC in toluene, respectively, Figs. 6-9). This can be atributed to the higher tendency of the grafted chitosan to retain water, which may be assigned to the:

i) increase in the number of hydrophilic groups from chitosan as a consequence of the supplementary polar groups (-COOH, -CH_2Cl) introduced in chitosan after the grafting polymerisation/copolymerisation of MA and VBC;

ii) supramolecular restructuring/reorganisation of chitosan following its pre-treatment with $Ce(SO_4)_2$ and the grafting polymerisation, which led to the breaking of some hydrogen bonds from chitosan and the generation of free -OH and -NH_2 groups, which became available for binding water molecules;

iii) water molecules involved in the formation of a complex between the Ce^{4+} ions and the - NH_2 and -OH groups from chitosan.

In all thermal analyses (Fig. 6-12), the first step of thermal degradation is accompanied by an endothermic peak in the DTA curves, which confirms that this step is associated with water evaporation from the chitosan sample.

The second thermal degradation step corresponds to the significant weight loss in the chitosan modified by the grafting homopolymerisation/copolymerisation of MA and VBC. Thus, for chitosan modified by grafting homopolymerisation of MA (Fig. 8), this step occurs between 149.09°C and 366.85°C and is accompanied by 46.7% weight loss. For chitosan modified by grafting homopolymerisation of VBC (Fig.7), this step occurs between 153.76°C and 352.16 °C and is accompanied by 43.35% weight loss. In the case of chitosan modified by grafting copolymerisation of MA and VBC in 1,4-dioxane (Fig.8.), this stage occurs between 141.5°C and 356.16°C and is characterised by a 48.01% weight loss (Fig.9.), while for the chitosan modified by grafting copolymerisation of MA and VBC in toluene, this step is between 150.66°C and 361.01°C and is accompanied by 47.27% weight loss. In all cases this thermal effect can be assigned to the thermal decomposition (by deacetylation and depolymerisation) and the thermo-oxidative degradation of chitosan of MA and VBC homopolymers/copolymer grafted on the chitosan chains, phenomena accompanied by the release of volatile compounds, formation of char, oxidation of the volatile compounds etc. Although in this step, as denoted by the

TGA curves, the weight loss is significant, in the corresponding DTA curves, only a minor exothermic peak can be seen, proof that in this step, the exothermic thermo-oxidative degradation processes are accompanied by intense endothermal thermal degradation processes.

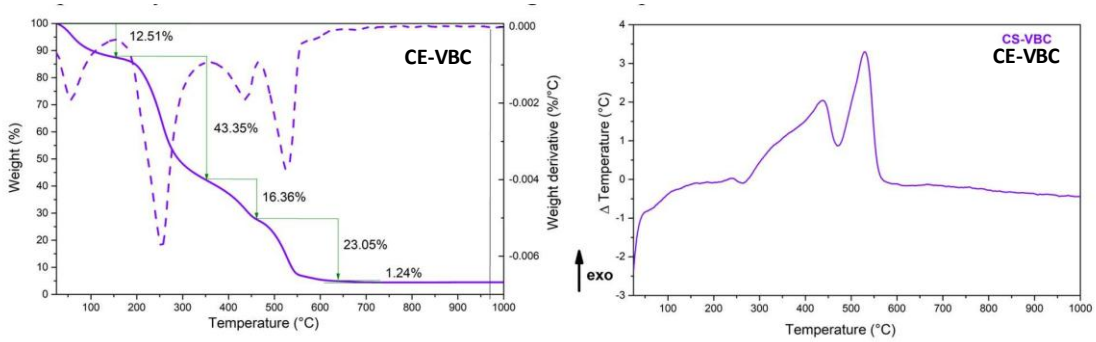

Fig. 7. The thermogravimetric (TG), derivative thermogravimetric (DTG) and differential thermal analysis (DTA) curves of chitosan modified by grafting homopolymerisation of VBC

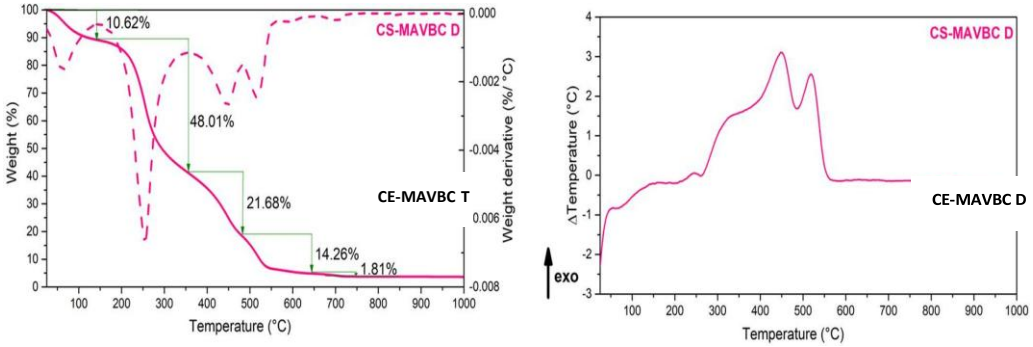

Fig. 8. The thermogravimetric and differential thermal analysis (DTA) of chitosan modified by grafted MA-VBC homopolymer in 1,4-dioxane (CE-MAVBC D)

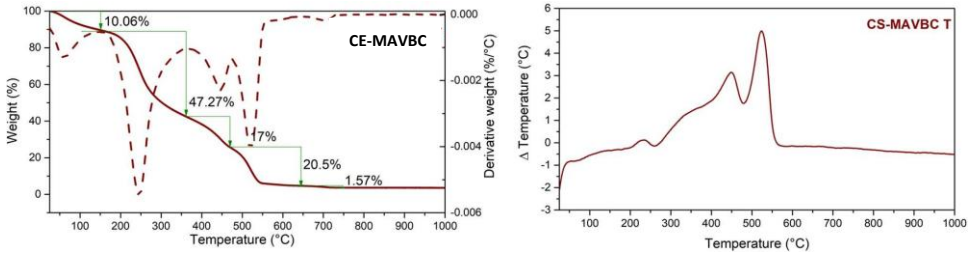

Fig. 9. The thermogravimetric and differential thermal analysis (DTA) of chitosan modified by grafted MA-VBC copolymer in toluene (CE-MAVBC T

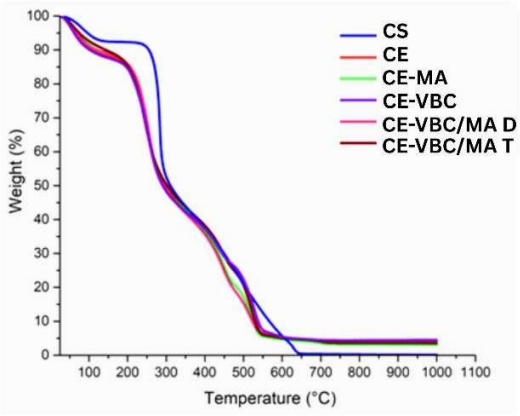

Fig. 10. Thermogravimetric analysis: (a) pure chitosan (CS) (b) Ce(SO4)2-treated chitosan (CE); (c) grafting homopolymerization of MA (CE-MA) (d) grafting homopolymerization of VBC (CE-VBC) (e) grafting copolymerization of MA and VBC in 1,4-dioxane (CE-MAVBC D) (f) grafting copolymerization of MA and VBC in toluene (CE-MAVBC T)

It is worth mentioning that this second step of thermal degradation existing in the chitosan modified by the grafting homopolymerisation/copolymerisation of MA and VBC starts much earlier than in the case of CE for which this degradation step starts at ~210°C as shown in Fig. 10..

This decrease in the thermal stability of the grafted chitosan may be due to

i) the introduction /formation of new groups/moieties with lower thermal stability in chitosan following its chemical modification by grafting polymerisation or following the initiation of the grafting polymerization;

ii) the existence of residual (not consumed) Ce^{4+} metal ions in the modified chitosan that act as catalysts for the thermal decomposition of chitosan. It is well known that Ce^{4+} ions are strong oxidising reagents, which can oxidise both the chitosan chains and the polymer/copolymer grafted on its chains, especially at higher temperatures [10];

iii) the coordination of the Ce^{4+} ions with the -NH_2 and -OH from chitosan, some of the hydrogen bonding interactions leading to a drop in the thermal stability of the grafted chitosan as compared to the unmodified chitosan.

Another noteworthy aspect is the higher temperature at which the second thermal degradation begins in the case of poly(VBC)-grafted chitosan as compared to chitosan modified by the grafting homopolymerisation of MA and grafting copolymerisation of MA and VBC (Fig. 10). This 5% increase in thermal stability of poly(VBC)-grafted chitosan may be attributed to the higher amount of VBC units attached to chitosan in this case, the aromatic rings of VBC possessing an inherent high thermal stability. The poly(VBC) graft may coat the chitosan surface, hence the higher thermal stability of the grafted chitosan in this case. The chains of the

grafted polymer may also entangle and form a physical crosslinked type of network which, during heating, includes an insulative carbonaceous char on the surface of the chitosan, which acts as a physical barrier for the

transfer of heat, oxygen, and decomposition products, delaying the thermal degradation and combustion of the material [11].

The third thermal degradation step corresponds to a significant weight loss in all grafted samples. Thus, for chitosan modified by grafting homopolymerisation of MA (Fig. 8), this step occurs between 366.85℃ and 456.09℃ and is accompanied by 13.29% weight loss whereas for chitosan modified by grafting homopolymerisation of VBC, this step occurs between 352.16℃ and 460.5℃ and is accompanied by 16.36% weight loss. In the case of chitosan modified by grafting copolymerisation of MA and VBC in 1,4-dioxane (Fig. 8.), this step occurs between

356.16℃ and 483.83℃ and is characterised by 21.68% weight loss, while for the chitosan modified by grafting copolymerisation of MA and VBC in toluene (Fig. 9), this step occurs between 361.01℃ and 472.77℃ and is accompanied by 17% weight loss.

The fourth thermal degradation step it is also accompanied with a significant weight loss in the chitosan modified by the grafting homopolymerisation/copolymerisation of MA (Fig. 8) and VBC (Fig. 7). Thus for the chitosan modified by the grafting homopolymerisation of MA, this step occurs between 456.09℃ and 637.96℃ and is accompanied by 23.59% weight loss whereas for chitosan modified by grafting homopolymerisation of VBC, this step take place between 460.5℃ and 640.02℃ and is accompanied by 23.05% weight loss. In the case of chitosan modified by grafting copolymerisation of MA and VBC in 1,4-dioxane (Fig. 8.), this step is observed between

483.83℃ and 643.83℃ and is characterised by a 14.26% weight loss, whereas for the chitosan modified by grafting copolymerisation of MA and VBC in toluene (Fig. 9.), this step is between

472.77℃ and 643.85℃ and is accompanied by 20.5% weight loss.

In the DTA curves (Fig. 10), these two steps of thermal degradation are associated with two exothermic peaks, a sign that more advanced thermo-oxidative degradation of chitosan and grafted polymer/copolymer, as well as more advanced thermo-oxidative degradation of various products formed in the first thermal degradation steps occur in these stages. The occurrence of these thermal degradation steps in chitosan modified by the graft homopolymerisation/copolymerisation of MA and VBC at approximately the same temperatures as in chitosan pre-treated with $Ce(SO4)2$ means that the chemical modification of functionalized chitosan with the homopolymers/copolymer of MA and VBC does not significantly alter the thermal stability of chitosan, responsible for this being rather the pre-treatment of chitosan with $Ce(SO4)2$. The existence of two degradation steps instead of a single

one, as is the case of pure chitosan in this temperature range, may be due to the $Ce(SO4)2$, which was not consumed in the grafting polymerisation reaction. Phenomena such as the thermal decomposition of ceric hydroxide ($Ce(OH)4$) or ceric sulphate ($Ce(SO4)2$), which are converted into ceric oxide ($CeO2$) or potential phase transitions of $CeO2$ may occur in addition to the thermo-oxidative degradation of the polymers and hence the differences between the TGA curve of pure chitosan and those of grafted chitosan.

A fifth final thermal degradation step can be observed for the chitosan modified by the grafting polymerisation/copolymerisation of MA/VBC. In the case of chitosan modified by the grafting polymerisation of MA (Fig. 8), this stage lies between 637.96°C and 722.5°C and corresponds to 1.78% weight loss, while for the chitosan modified by the grafting polymerisation of VBC (Fig. 7), this step occurs between 640.02°C and 731.48°C and is associated with a 1.24% weight loss. In the case of chitosan modified by the grafting copolymerisation of MA and VBC in 1,4-dioxane (Fig. 8.), this step lies between 643.83°C and 748.33°C and is accompanied by a 1.81% weight loss, whereas for the chitosan modified by the grafting copolymerisation of MA and VBC in toluene (Fig. 9.), this step occurs between 643.58°C and 748.66°C and is accompanied by a 1.57% weight loss. As it can be seen, this step is characterised by a minor weight loss and it can

be attributed to the thermo-oxidative degradation of residual carbon resulting from the previous thermal degradation steps.

3.3. Raman Spectroscopy

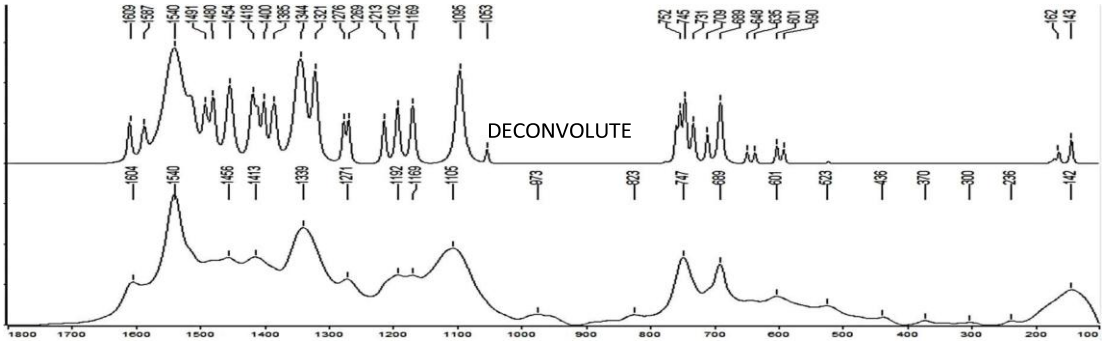

Fig. 11. Raman spectra of chitosan grafted with maleic anhydride (CE-AM)

Fig. 11 presents the Raman spectrum as well as the deconvoluted spectrum of CE-AM and highlights structural modifications induced by the grafting process. The spectral analysis reveals significant variations compared to native chitosan, particularly in the characteristic vibrational modes associated with amine and carbonyl functionalities. The NH_2 bending vibration at approximately 1604 cm^{-1}

shows a reduced intensity, indicating successful grafting of maleic anhydride onto the chitosan backbone. Additionally, the emergence of a strong peak around 1710 cm^{-1} corresponding to C=O stretching confirms the incorporation of maleic anhydride. Changes in the polymer backbone are further evidenced by the presence of C-H bending and deformation vibrations in the 1200-1300 cm^{-1} region. The aromatic ring vibrations observed in the 1000-1100 cm^{-1} range suggest interactions between the maleic anhydride and chitosan, further reinforcing the chemical changes induced by the grafting process. The broad spectral features between 500 and 800 cm^{-1} support the structural modifications, reflecting changes in the polymeric network. The overall spectral shifts and intensity variations validate the findings obtained from FTIR spectroscopy and Raman, confirming the successful chemical modification of chitosan through the grafting of maleic anhydride.

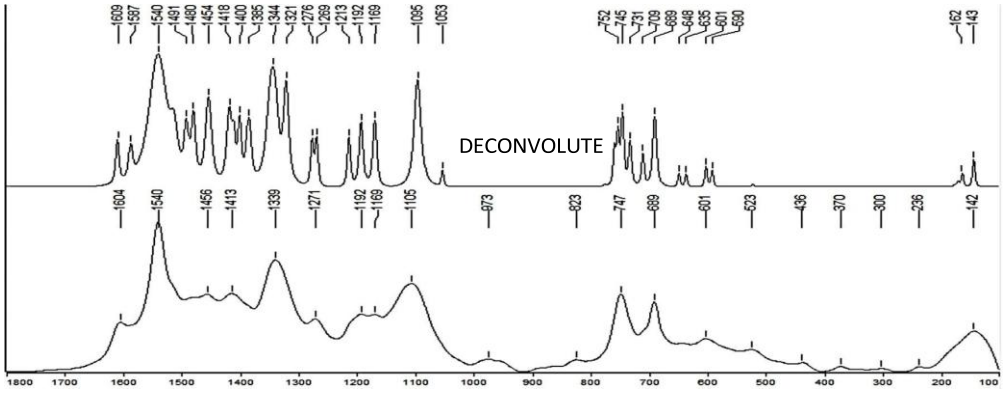

Fig. 12. Raman spectra of chitosan grafted with VBC (CE-VBC)

Fig. 12 presents the Raman Spectrum as well as the deconvoluted spectrum of CE-VBC and demonstrates the incorporation of aromatic functionalities onto the polymeric backbone. The spectral profile shows significant peaks corresponding to the characteristic vibrations of benzyl groups, with prominent signals in the region of 1000-1200 cm^{-1} indicative of aromatic C-H bending. The emergence of peaks around 1600 cm^{-1} suggests interactions between the grafted VBC and chitosan's functional groups, while additional shifts in the 1200-1500 cm^{-1} range indicate structural rearrangements due to polymerisation. The presence of bands in the 600-900 cm^{-1} range confirms the successful modification, consistent with the spectral features of benzylated compounds. The intensity variations and peak shifts corroborate with the findings from complementary FTIR spectroscpy and Raman spectra, confirm the effective grafting of vinyl benzyl chloride onto the chitosan backbone.

Fig. 13 reveals the Raman Spectra as well as the deconvoluted spectrum for CE-MA-VBC and provides insights into the combined structural effects of both

monomers. The spectral profile reveals significant shifts in key vibrational regions, demonstrating the synergistic impact of MA and VBC on chitosan's chemical structure. The NH_2 bending vibration observed at 1604 cm^{-1} in chitosan is noticeably altered, suggesting extensive interaction between the copolymer and the chitosan backbone. The strong carbonyl stretching band at 1710 cm^{-1}, characteristic of maleic anhydride grafting, remains evident, indicating successful incorporation of MA, while, the band corresponding to aromatic ring vibrations between 1000-1100 cm^{-1} and C-H bending in the 1200-1300 cm^{-1} range confirm the presence of VBC. The spectral features in the 600-900 cm^{-1} region further substantiate the copolymerisation process, demonstrating that both monomers have effectively grafted onto the chitosan structure. The overall spectral characteristics showed in Fig. 13 align with the observations from Figs. 12 and 13, validating the formation of a well-integrated MA-VBC copolymer on chitosan

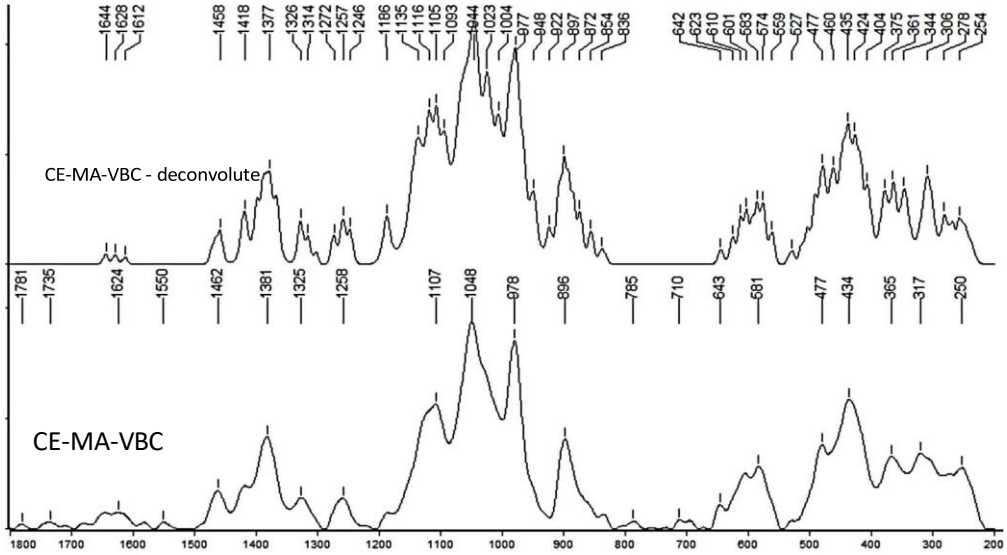

Fig. 13. Raman spectra of chitosan grafted with the MA-VBC

4. Conclusions

This study successfully demonstrated the graft polymerization of MA or VBC as well as the graft copolymerisation of maleic anhydride and 4-vinyl benzyl chloride onto chitosan using $Ce(SO_4)_2$ as an initiator. The efficiency of the grafting process was confirmed through spectroscopic and thermal analyses, which provided comprehensive insights into the structural and thermal modifications of the functionalised chitosan.

Raman spectroscopy confirmed significant spectral shifts a proof of the chemical modifications, including vibrational changes in amine, carbonyl, and

aromatic groups, thereby validating the successful attachment of both monomers. FTIR analysis supported these findings by identifying characteristic peaks corresponding to the new functional groups introduced by the polymerization or copolymerisation process. The thermogravimetric analysis (TGA) demonstrated alterations in the degradation profile of the modified chitosan, with an improvement in thermal stability, particularly for the chitosan grafted with VBC.

The grafting efficiency analysis indicated that VBC exhibited superior polymerisation behaviour compared to MA, which enhanced the structural integrity and the thermal performance. These findings establish the potential of MA-VBC grafted chitosan as an advanced functional biomaterial with potential applications in pharmaceuticals, and environmental science. The study provides valuable insights into the controlled modification of chitosan, opening avenues for its practical utilisation in industrial and biomedical fields.

REFERENCES

[1] *Bhattacharya, A., & Misra, B. N.*, Grafting: a versatile means to modify polymers: techniques, factors, and applications. Progress in Polymer Science, **29(8)**, 767–814, 2004.

[2] *Vega-Hernández, M. Á., et al*., A Review on the Synthesis, Characterization, and Modeling of Polymer Grafting. Processes, **9(2)**, 375, 202.

[3] *Caner, H., Hasipoğlu, H., Yılmaz, O., & Yılmaz, E.* (1998). Graft copolymerization of 4-vinylpyridine onto chitosan—I. By ceric ion initiation. European Polymer Journal, **34(4–5)**, 493–497, 1998.

[4] *Prashanth, K. V. H., & Tharanathan, R. N*., Studies on graft copolymerization of chitosan with synthetic monomers. Carbohydrate Polymers, **54(3)**, 343–35, 2003.

[5] *Pourjavadi, A., Mahdavinia, G. R., et al.*, Modified chitosan. I. Optimized cerium ammonium nitrate-induced synthesis of chitosan-graft-polyacrylonitrile. Journal of Applied Polymer Science, **88(8)**, 2048–2054, 2003.

[6] *Huang, M., Shen, X., & Sheng, Y.,* Study of graft copolymerization of N-maleamic acid-chitosan and butyl acrylate by gamma-ray irradiation. International Journal of Biological Macromolecules, **36(1–2)**, 98–102, 2005.

[7] *Liu, L., Chen, X. W., Wang, P., & Wang, C.,* Studies on methyl methacrylate grafted onto chitosan by ceric ion initiation. Advanced Materials Research, **284–286**, 1713–1716, 2011.

[8] *Mun, G. A., Nurkeeva, Z. S., et al*., Studies on graft copolymerization of 2-hydroxyethyl acrylate onto chitosan. Reactive and Functional Polymers, **68(3)**, 389–395, 2008.

[9] *M. Jaymand*, Synthesis and characterization of well-defined poly (4-chloromethyl styrene-g-4-vinylpyridine)/TiO2 nanocomposite via ATRP technique, doi: 10.1007/s10965-011-9566-x.

[10] *T. M. Don, C. F. King, and W. Y. Chiu*, Synthesis and properties of chitosan-modified poly(vinyl acetate), Journal of Applied Polymer Science, **vol. 86**, no. 12, pp. 3057–3063, Dec. 2002, doi: 10.1002/APP.11329.

[11] *E. Rezvani Ghomiet al.,* The Flame Retardancy of Polyethylene Composites: From Fundamental Concepts to Nanocomposites, Molecules 2020, **Vol. 25**, Page 515, 2020, doi: 10.3390/MOLECULES25215157